Brazilian Journal of Biology®

ISSN 1519-6984 (Print)
ISSN 1678-4375 (Online)

Original Article

Calotropis procera (L.) mediated synthesis of AgNPs and their application to control leaf spot of *Hibiscus rosa-sinensis* (L.)

Calotropis procera (L.) mediada pela síntese de AgNPs e sua aplicação no controle da mancha foliar de *Hibiscus rosa-sinensis* (L.)

R. Nawab[a], M. Ali[a], U. Haroon[a], A. Kamal[a], M. Akbar[a], F. Anwar[a], J. Ahmed[a], H. J. Chaudhary[a], A. Iqbal[b], M. Hashem[c, d], S. Alamri[c], H. A. S. ALHaithloul[e] and M. F. H. Munis[a*]

[a]Quaid-i-Azam University, Faculty of Biological Science, Department of Plant Sciences, Islamabad, Pakistan
[b]Quaid-i-Azam University, National Centre for Physics, Islamabad, Pakistan
[c]King Khalid University, College of Sciences, Department of Biology, Abha, Saudi Arabia
[d]Assiut University, Faculty of Sciences, Botany and Microbiology Department, Assiut, Egypt
[e]Jouf University, College of Science, Biology Department, Sakaka, Saudi Arabia

Abstract

Nature is gifted with a wide range of ornamental plants, which beautify and clean the nature. Due to its great aesthetic value, there is a need to protect these plants from a variety of biotic and abiotic stresses. *Hibiscus rosa-sinensis* (L.) is an ornamental plant and it is commonly known as China rose or shoeblack plant. It is affected by several fungal and bacterial pathogens. Current study was designed to isolate leaf spot pathogen of *H. rosa-sinensis* and its control using silver nanoparticles (AgNPs). Based on molecular and morphological features, the isolated leaf spot pathogen was identified as *Aspergillus niger*. AgNPs were synthesized in the leaf extract of *Calotropis procera* and characterized. UV-vis spectral analysis displayed discrete plasmon resonance bands on the surface of synthesized AgNPs, depicting the presence of aromatic amino acids. Fourier transform infrared spectroscopy (FTIR) described the presence of C-O, NH, C-H, and O-H functional groups, which act as stabilizing and reducing molecules. X-ray diffraction (XRD) revealed the average size (~32.43 nm) of AgNPs and scanning electron microscopy (SEM) depicted their spherical nature. In this study, *in vitro* and *in vivo* antifungal activity of AgNPs was investigated. *In vitro* antifungal activity analysis revealed the highest growth inhibition of mycelia (87%) at 1.0 mg/ml concentration of AgNPs. The same concentration of AgNPs tremendously inhibited the spread of disease on infected leaves of *H. rosa-sinensis*. These results demonstrated significant disease control ability of AgNPs and suggested their use on different ornamental plants.

Keywords: *Calotropis procera*, AgNPs, FTIR, SEM, *Hibiscus rosa-sinensis*.

Resumo

A natureza é presenteada com uma grande variedade de plantas ornamentais que embelezam e limpam a natureza. Por causa de seu grande valor estético, existe a necessidade de proteger essas plantas de uma variedade de estresses bióticos e abióticos. *Hibiscus rosa-sinensis* (L.) é uma planta ornamental comumente conhecida como rosa-da-China ou graxa-de-estudante. É afetada por vários patógenos fúngicos e bacterianos. O presente estudo buscou isolar o patógeno da mancha foliar de *H. rosa-sinensis* e seu controle usando nanopartículas de prata (AgNPs). Com base nas características moleculares e morfológicas, o patógeno isolado da mancha foliar foi identificado como *Aspergillus niger*. As AgNPs foram sintetizadas no extrato de folhas de *Calotropis procera* e caracterizadas. A análise de espectroscopia UV-vis mostrou discretas bandas de ressonância plasmônica na superfície das AgNPs sintetizadas, mostrando a presença de aminoácidos aromáticos. A espectroscopia no infravermelho com transformada de Fourier (FTIR) descreveu a presença de grupos funcionais C-O, NH, C-H e O-H, que atuam como moléculas estabilizadoras e redutoras. A difração de raios X (DRX) revelou o tamanho médio (~32,43 nm) das AgNPs e a microscopia eletrônica de varredura (MEV) mostrou sua natureza esférica. Neste estudo, foi investigada a atividade antifúngica *in vitro* e *in vivo* de AgNPs. A análise da atividade antifúngica *in vitro* revelou a maior inibição do crescimento de micélio (87%) na concentração de 1,0 mg/ml de AgNPs. A mesma concentração de AgNPs inibiu a propagação da doença em folhas infectadas de *H. rosa-sinensis*. Esses resultados demonstraram significativa capacidade de controle de doenças das AgNPs e sugeriram seu uso em diferentes plantas ornamentais.

Palavras-chave: *Calotropis procera*, AgNPs, FTIR, SEM, *Hibiscus rosa-sinensis*.

*e-mail: munis@qau.edu.pk
Received: February 18, 2022 – Accepted: April 23, 2022

1. Introduction

Ornamental plant diseases are prevalent around the world. These diseases are caused by several pathogenic fungi in different parts of the world (Anvar et al., 2021). Gardens and parks hold a unique position in preserving the ornamental plants, which play significant role in enhancement of natural beauty and decreasing the pollution, caused by anthropogenic activities. In this scenario, it is very important to protect ornamental plants from variety of pathogens *Hibiscus rosa-sinensis* (L.), locally known as China rose and Gul-e-zban-daraz, is an annual and perennial plant. It belongs to family Malvaceae and it is native to Pakistan, China, India, Sri Lanka, Nigeria and Southeast Asia (Shelke et al., 2021). *H. rosa-sinensis* (L.) has a lot of applications in pharmacology, medicines, beverages and cosmetics (Sivaraman and Saju, 2021). Phyto-constituents like flavonoids, phenols, sterols, tannins, glucosides, anthocyanin and lignin are present in *H. rosa-sinensis* (Kapoor et al., 2021), and testified as pain-relieving, antipyretic, anti-asthmatic, anti-inflammatory (Begum et al., 2015), cardio-protective (Khandelwal et al., 2011) and wound healer (Sharma et al., 2021). Several fungal pathogens including *Cercospora hibisci-manihotis* (Ghosh et al., 2009), *Pseudomonas cichorii*, *Pseudomonas syringae*, *Xanthomonas campestris* (Chase, 1986) and *Fusarium oxysporum* have been reported to causes leaf spots of *H. rosa-sinensis* (Lecomte et al., 2016).

In ornamental plants, about 70% of biotic diseases are caused by fungi, which result in significant losses (Khan et al., 2021). Pathogenic fungal species produce toxins, that disturb normal metabolic activities in plant tissues (Punja, 2006). Most of the plants fungi are saprophytic while some others are bio-trophic and necrotrophic that cause diseases on their respective hosts (Dey, 1978). Obligate bio-trophic fungi grow on living hosts and in return cause ornamental plant diseases like leaf spots, blights, rusts, smuts, powdery mildew, and downy mildew. Fungal diseases are traditionally controlled with chemical fungicides, which are helpful only for specific diseases. Excessive use of fungicide causes hazardous human health and environmental consequences. Synthetic compounds, used in agriculture to control plant pathogens, are genotoxic to humans (Cohn et al., 2007). Fungicide application during bloom may limit pollination by reducing pollen deposition and insect foraging performance (Tamburini et al., 2021). Once the infection spreads, the commodity becomes unsuitable for commercialization. Due to negative consequences of chemicals on animals, human health, and the environment, several plant pathologists have focused on establishing novel alternatives for the management of plant pathogens. An integrated strategy can give the best results for disease prevention, in which biological control can enhance the ornate selection for resistance (Lecomte et al., 2016).

Application of nanotechnology in agriculture has shifted the momentum and nanomaterials are gaining importance in plant disease management (Pinto et al., 2019). With the outburst of antibiotic resistance in bacteria and fungi, more focus is being given on developing new antimicrobial agents. Metallic nanoparticles have been reported to exhibit enhanced antimicrobial capabilities (Amin et al., 2020). Nanoscale materials display excellent antimicrobial agents because of their large surface area to volume ratio, and distinctive physical and chemical attributes. The terminology of "nanotechnology" was proposed by Norio Taniguchi in 1974 (Taniguchi, 1974). Nanoparticles (NPs) typically ranging from 1 to 100 nanometers (nm), are being used as anti-microbial agents (Madkour, 2019). In green synthesis of nanoparticles, plant extracts are used to produce nanoparticles for biological applications in a sustainable, biocompatible, and environment friendly way (Razavi et al., 2015). Plant extracts are more appropriate for the synthesis of NPs and plant phyto-constituents also function as both reducing and capping agents (Hamelian et al., 2018). Green synthesis is less time consuming and more economical (Aravind et al., 2021). Due to distinctive anti-microbial properties, silver nanoparticles (AgNPs) have been extensively employed in numerous pharmacological and biological applications. AgNPs are environment friendly, sustainable, easy to process, cost effective, and nontoxic (Bao et al., 2021). Like other medicinal plants, *Calotropis procera* (L.) possesses antimicrobial, anti-coagulant, parasiticidal, purgative, anti-inflammatory and diuretic properties and it is being used in ethno-veterinary medicine system of Pakistan (Silva et al., 2010). *C. procera* (L.) leaf extract has been successfully used to synthesize NPs due to presence of phytochemicals like fatty acid, ethyl ester, linoleic amino acids (Pattnaik et al., 2017), phenolic compounds, flavonoid contents and terpenoids (Kainama et al., 2020).

Current study has been designed to synthesize AgNPs in the extract of *C. procera* (L.) and analyze their antifungal activity potential to control leaf spot disease of *H. rosa-sinensis*.

2. Materials and Methods

2.1. Chemicals and reagents

Chemicals utilized in experiment work were of analytical reagent grade and were bought from Sigma Aldrich (Germany).

2.2. Sample collection

Diseased leaf samples of *H. rosa-sinensis* (L.) were collected from the parks of Quaid-i-Azam University, Islamabad, during August-September 2021. Diseased leaf samples were collected randomly and separately kept in sterilized polythene bags, labeled and brought to the laboratory for further study.

2.3. Isolation of disease-causing pathogen

For isolating pathogen from the infected leaf samples, tissue planting method was used. Infected sample was surface sterilized with 70% ethanol for two minutes. Disinfected leaf sample was cut from the infected portion with the sterilized blade and placed in the Petri plate of potato dextrose agar (PDA) containing medium. Petri plates were sealed with Parafilm™ and incubated for seven days

at 27° C. To get pure culture, the mycelia from the edges of fungal colony was transferred to PDA plates. After seven days of incubation of the pure culture, cultural traits were observed on PDA plates.

2.4. Microscopic identification of pathogen

For identification, hyphae and reproductive structures of isolated fungus were examined under light microscope. Few drops of lactic acid and lacto-phenol blue were positioned on slide. Mycelium were picked from edges of fungal culture and placed on the slide. Cover slip was carefully placed, avoiding air bubbles and the slide was observed under light microscope at 100 × magnification.

2.5. Molecular identification of pathogen

Fungal DNA was isolated, following a standard method (Jin et al., 2004). Polymerase chain reaction (PCR) with CMD5/CMD6 primers was performed to amplify the calmodulin (CaM) gene (Susca et al., 2007). Similarly, the tubulin gene was also amplified using tubulin primers (Bt2a/Bt2b) (Liaquat et al., 2019). In the reaction mixture, genomic DNA (1 µl), *Taq* DNA polymerase (1.5 µl), dNTPs (6 µl), 10× polymerase buffer (5 µl), and each primer (1 µl) were used. Reaction was performed at 94°C for 4 minutes, followed by 32 cycles of 94° C for 60 seconds, 58° C for 1 minute, and 72 °C for 60 seconds. The PCR was maintained at 72 °C for 10 minutes after 35 cycles for terminal extension. Product of PCR was sequenced and used for BLAST analysis on NCBI database (http://www.ncbi.nlm.nih.gov). MEGA 7.0, was used to align nucleotide sequences (Tamura et al., 2004) and phylogenetic tree was constructed with 1,000 bootstrap replications.

2.6. Pathogenicity test

Koch's postulates were followed to confirm the pathogenicity of isolated fungus (Khizar et al., 2020). The fungus was grown for seven days on PDA media. Isolated pure fungal culture was inoculated on healthy leaves of *H. rosa-sinensis*. The inoculated leaves were placed in petri plate at 25 °C. After 3–4 days of incubation, leaf spot symptoms were observed. The disease-inducing pathogen was re-isolated on PDA media, from the infected leaves, and compared with initially isolated pathogen.

2.7. Preparation of plant extract

Fresh leaves of *C. procera* were washed with distilled water and dried in shade at room temperature. Dry leaves were grinded to fine powder, using a blender. Leaf powder (20 g) was dissolved in water (500 ml) and kept at 80 °C for 30 minutes in water bath. Solution was cooled down at room temperature and filtered using muslin cloth and sterilized Whatman filter paper no. 1 to obtain aqueous extract. The pH of plant extract was recorded and stored at 4 °C, till further use.

2.8. Synthesis of silver oxide nanoparticles

For the synthesis of AgNPs, 100 ml of *C. procera* extract was mixed with 100 ml of 1 mM $AgNO_3$ (1:1) in 500 ml Erlenmeyer flask at 25 °C. After combining plant extract with $AgNO_3$ solution, a color shift was detected. The flask was placed on hot plate stirrer for 2 hours at 70 °C and 150 rpm. Mixture was centrifuged at 6000 rpm for 10 minutes and the obtained pellet was re-suspended in 70% ethanol to remove any interactive biomolecule. This procedure was repeated thrice to ensure enhanced separation of AgNPs. The sample was then calcined by placing in a hot furnace at 500° for 3 h. This high temperature treatment produced nanoparticles in the form of fine powder.

2.9. Characterization of silver oxide nanoparticles

Synthesized nanoparticles were characterized by the following analyses.

2.10. UV-vis spectral analysis

The reduction of silver oxide NPs by leaf extract was monitored by evaluating the UV-vis spectra of the solution with UV-vis spectrophotometer (Shimadzu model UV-1601) in 200-350 nm range.

2.11. Fourier transform infrared spectroscopy (FTIR) spectrophotometer

FTIR spectra of AgNPs was obtained to determine the presence of different functional groups on synthesized AgNPs. Infrared (IR) spectra were recorded using FTIR Spectrometer (Model No. FTSW 300 MX, BIO-RAD, California, USA) with 4 cm^{-1} resolution.

2.12. X-ray Diffraction (XRD) analysis

X-ray diffraction (XRD) technique was carried out by using Bruker, *D8 advance* at the scan range of 10°-80°. The XRD was operated with CuK_α radiation source (λ=1.54056Å), generated at 40 kV and 40 mA. The average crystal particle size was calculated using Debye–Scherrer's formula (Equation 1).

$$D = k\lambda / \beta Cos\theta \quad (1)$$

Where: k = constant; λ-= wavelength of X-Ray; D = average crystalline size; B = Full width half maximum (Wang, 2000).

2.13. Scanning Electron Microscopy (SEM)

Morphology of AgNPs was determined by Scanning electron microscopy (JSM5910, JEOL Japan) and images were obtained.

2.14. Antifungal activity of AgNPs, in vitro

For antifungal activity analysis, PDA media was amended with different concentrations of AgNPs viz. 1.0 mg/ml, 0.75 mg/ml, 0.5 mg/ml, 0.25 mg/ml, and 0.1 mg/ml. Cork borer was used to excise and place the fungus in center of AgNPs amended media plates. Media without NPs served as control. Inoculated plates were placed in an incubator at 27 ° C for 7 days and zones of inhibition were calculated by the following formula (Equation 2):

$$Growth\ inhibition\ percentage = \left(C - T\right) / C \times 100 \quad (2)$$

Where, C = Average mycelial growth in control Petri disease; T = Average mycelial growth in AgNPs amended Petri dishes.

2.15. Antifungal activity of AgNPs, in vivo

In this experiment, nine healthy plants of *H. rosa-sinensis* were used in three treatments. Three plants of first control treatment (T_1) were neither treated with fungus nor with nanoparticles. While six plants of other two treatments (T_2 and T_3) were spray inoculated with a known spore suspension (1×10^5 spores per ml). All the plants were covered with polythene bags. After two days of inoculation, T_2 treatment was left undisturbed while T_3 treatment was sprayed with 1 mg/ml concentration of AgNPs. Plants of T_3 treatment were sprayed thrice with AgNPs, on alternate days. All the plants were kept in green house at 25 °C and 90% relative humidity for one week and symptoms were recorded, thereafter.

2.16. Estimation of physiological and biochemical changes

After one week of inoculation, following parameters were studied:

2.17. Osmo-protectants

For the determination of proline content, a standard protocol was followed (Bates et al., 1973). At 520 nm, the absorbance of the mixture was recorded, and the amount of proline was calculated. Using the method of Hahm et al. (2017) total sugar contents were measured. Total soluble sugar contents were quantified using a standard curve (spanning from 0 to 10 mg of dextrose sugar) and the optical density was determined at 620 nm. Standard protocol was used to determine total protein content (Lowry et al., 1951). As a standard phosphate buffer, bovine serum albumin was used (stock solution).

2.18. Photosynthetic pigments

Fresh leaves (0.1 g) were grinded in 80% acetone and placed in the dark for 24 hours. The absorbance for chlorophyll a (at 645 nm), chlorophyll b (at 663 nm) and carotenoids (at 480 nm) were calculated (Hassanzadeh et al., 2009; Stockburger and Mitchell, 1999).

2.19. Relative electrolytic leakage and relative water content

Relative electrolytic leakage (REL) was calculated by the standard method of Lutts et al. (1996). The relative water contents (RWC) of leaves were determined by first determining the fresh weight (FW) of leaves. These leaves were placed in water for 24 hours and its turgid weight (TW) was determined. Leaves were dried in hot air oven and their dry weight (DW) was determined. Relative water contents were derived by the following formula (Weatherley, 1950) (Equation 3):

$$RWC = FW - DW \,/\, TW - DW \times 100 \quad (3)$$

2.20. Antioxidant enzyme assay

Protocol of Beauchamp and Fridovich (1971) was followed to determine the amount of Superoxide Dismutase (SOD). Activity of peroxidase (POD) was determined by the protocol of (Vetter et al., 1958) with little modifications (Gorin and Heidema, 1976)

2.21. Statistical analysis

The experiments were carried out in triplicates, unless otherwise described. The means and standard errors were determined using Excel 2016. Using Statistix version 8.1, one-way ANOVA was performed, followed by Tukey's least significant difference analysis.

3. Results

3.1. Identification of pathogen and analysis of its pathogenicity

In the gardens of university, small, blackish, round spot was observed on the leaves of *H. rosa-sinensis* (Figure 1a). Diseased parts were placed on PDA and after 7 days of incubation, white to yellow mycelial mat was observed. With the maturation of conidia, these mycelia turned black, rapidly (Figure 1b). On the back side of Petri plate, the mycelia were white to pale (Figure 1c). These features depicted this pathogen to be *Aspergillus niger*. Microscopic observations at 100× magnification displayed large dark brown conidia and conidiophores turned dark towards vesicles. Conidiophores formed septate hyphae (Figure 1d). Koch's postulates successfully described the pathogenicity of isolated pathogen. Initial symptoms appeared after three days of inoculation (Figure 1e). These symptoms spread further and resembled with typical field symptoms, after one week of inoculation (Figure 1f). Fungus was isolated from these self-infected leaves and grown on PDA media. After 3-4 days, similar fungal morphology was observed (Figure 1g-1h).

BLAST analysis of obtained sequence showed 100% similarity with *A. niger* (Accession no. JN587346.1). Phylogenetic tree efficiently depicted evolutionary relationship and showed the presence of these two sequences in the same clade as shown in Figure 2.

3.2. UV-vis spectral analysis

UV-vis spectroscopy revealed the synthesis of AgNPs by displaying discrete surface plasmon resonance bands with a peak centered around 271 nm (Figure 3). This absorption band depicted the presence of proteins (aromatic amino acids) and showed the electronic excitations in tryptophan and tyrosine of protein molecules (Ahmad et al., 2011).

3.3. Fourier Transform Infrared Spectroscopy (FTIR)

FTIR was employed to examine the significance of stabilizing and reducing proficiency of *C. procera* extract. FTIR peaks were observed at 1116, 1384, 1606, 2361, 2804, 2923, 3315 and 3421 cm^{-1} (see Figure 4). FTIR spectrum confirmed the presence of alkanes, alcohol, and primary and secondary amides of proteins. Peak at

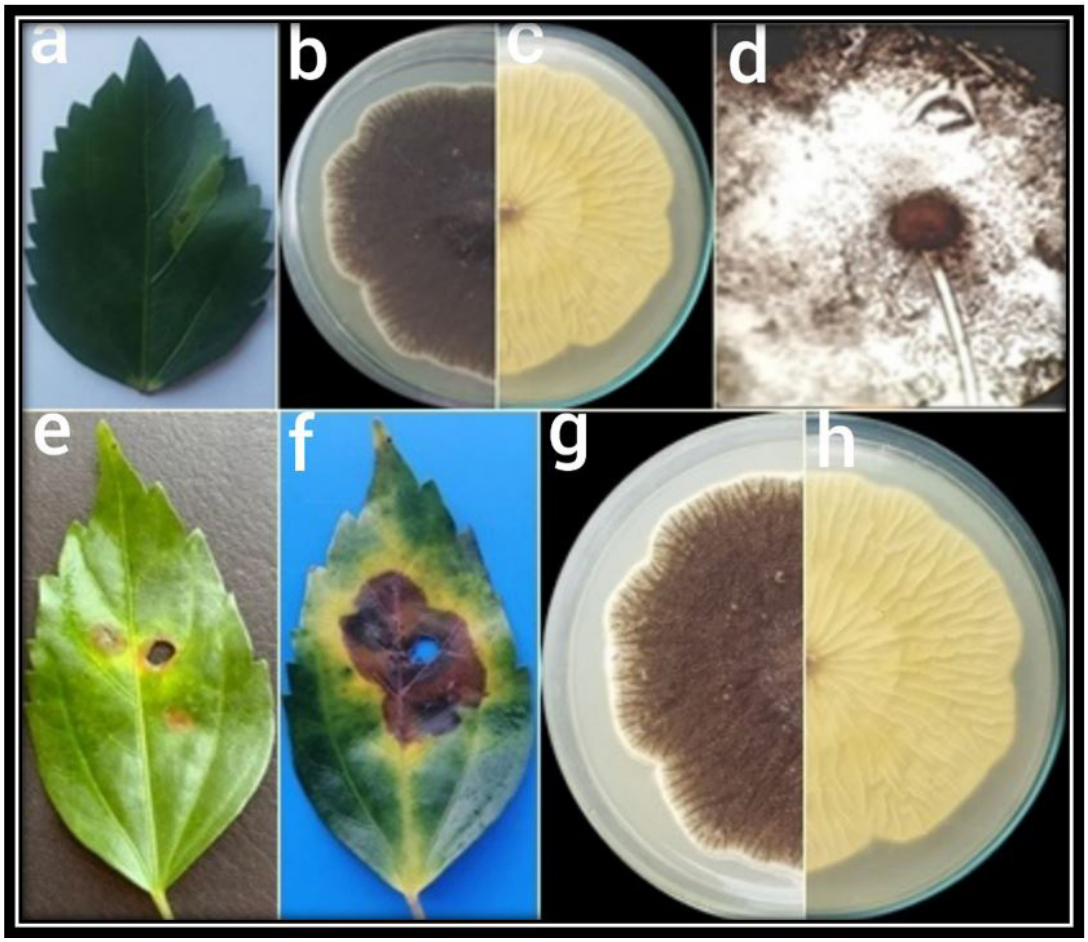

Figure 1. Spots were observed on the leaves of *H. rosa-sinensis* (a). Disease causing fungus was isolated on PDA and observed from front side (b) and back side (c) of Petri plate. Fungus was observed under light microscope at 100× magnification (d). Disease symptoms were observed after 3 days (e) and 7 days post inoculation (f). Pathogen was re-isolated and petri plates were observed from front (g) and back side (h).

1116 cm^{-1} indicated strong C-O stretch (alcohol), while bands at 2361, 2923 and 3421 cm^{-1} revealed NH stretching vibrations of primary and secondary amides of proteins (Ali and Abdallah, 2020). The band at 1384 cm^{-1} described C-H bending (Mohamed et al., 2014) while prominent band at 1606 cm^{-1} represented N-H stretching (amide group), which can reduce $AgNO_3$ to Ag (Sanci and Volkan, 2009). Peaks at 2804 cm^{-1} and 3315 cm^{-1} corresponded to –CH (alkane) and O-H groups (alcohol), respectively (Verma and Bharadvaja, 2021).

3.4. X-ray Diffraction (XRD) analysis

XRD analysis successfully demonstrated the nature of AgNPs as shown in Figure 5. The peak positions were consistent with metallic silver. This method was based on projecting a monochromatic X-ray beam onto the material at theta (θ) angle. Several Bragg reflections with 2θ values of 37.79°, 43.98°, 64.13° and 77.09° were obtained (see Figure 5). The Full Width at Half Maximum (FWHM) was measured for planes of reflection (111, 200, 220 and 311) and used in Debye–Scherrer equation to calculate the size of NPs. Average size of ~ 32.43 nm of green silver oxide NPs was calculated. The strong and sharp peaks revealed crystalline nature of AgNPs (Aravind et al., 2021). The observed XRD pattern was similar to JCPDS: 87–0720. All reflectance patterns showed a pure and polycrystalline face-centered cubic structure of pure silver metal (Parvathi et al., 2020). Additionally, some undesired peaks were also noticed, suggesting the crystalline organic phase of AgNPs.

3.5. Scanning Electron Microscopy (SEM)

SEM examination further revealed predominantly spherical and well-defined shape of AgNPs as shown in Figure 6. Varying particle sizes may be linked to diverse forms. Some were present in agglomerations due to drying process of the samples (Safa et al., 2021).

3.6. Antifungal assay, in vitro

A variable growth inhibition was observed at different concentration of AgNPs (see Figure 7; Table 1). Maximum

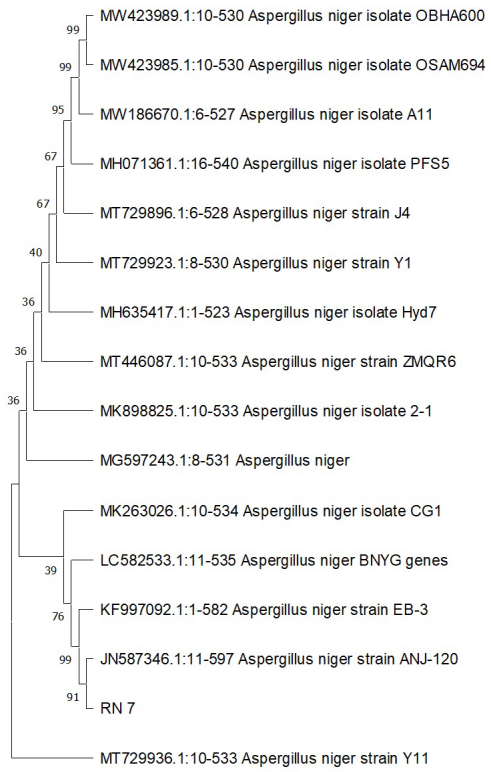

Figure 2. Phylogenetic analysis of isolated pathogen.

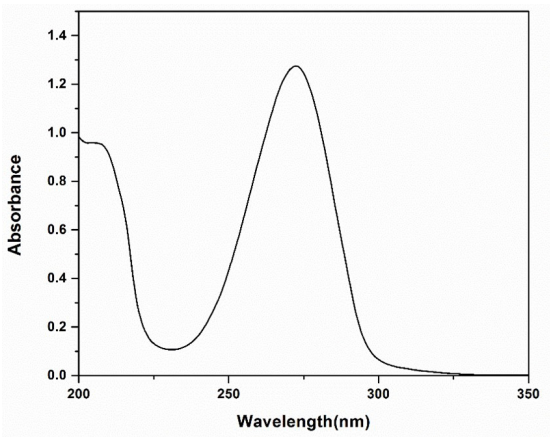

Figure 3. UV/Vis of AgNPs, showing the synthesis of AgNPs.

growth inhibition (87%) was measured at 1.0 mg/mL concentration of AgNPs. Our findings further declared that even at low concentrations of NPs (0.1 mg/mL), mycelial growth can be significantly inhibited.

3.7. Disease control assay, in vivo

Application of AgNPs gave amazing results to control leaf spot of *H. rosa-sinensis.* In AgNPs treated plants (T_3), no disease symptoms were observed (see Figure 8a) while

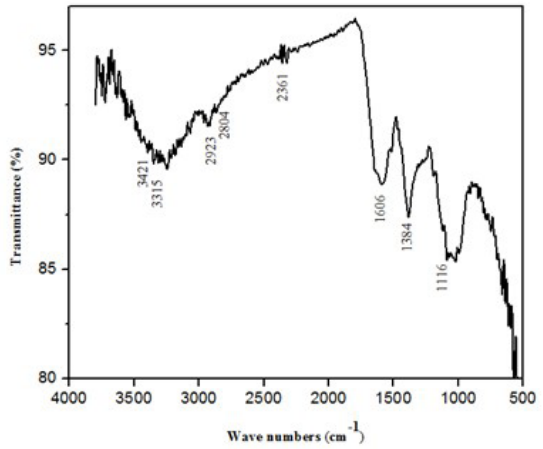

Figure 4. FTIR spectra of *C. procera* mediated AgNPs.

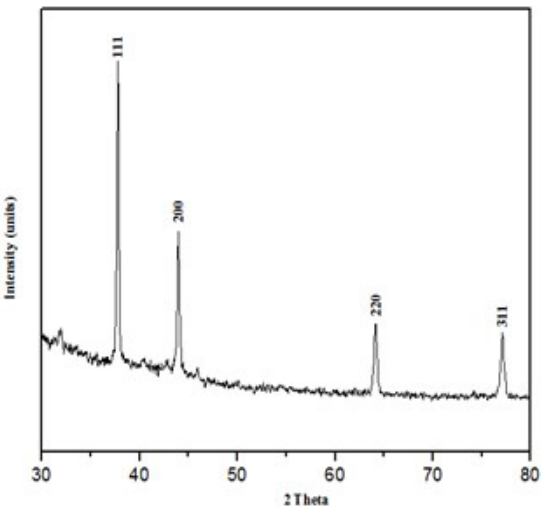

Figure 5. XRD analysis of *C. procera* mediated AgNPs.

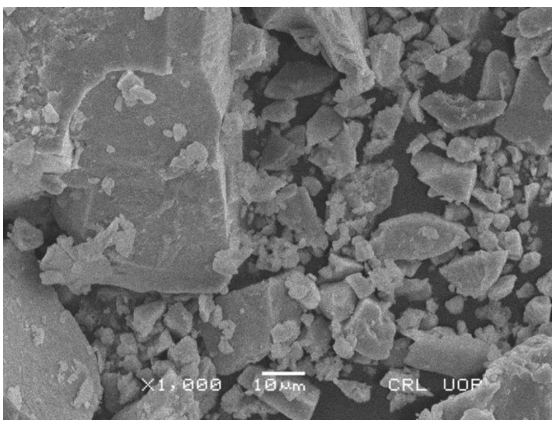

Figure 6. SEM of *C. procera* mediated AgNPs.

inoculated plants (T_2) displayed significant damage to the leaves (Figure 8b). Inoculated plants displayed blackish, round and necrotic leaf spots (Figure 8c).

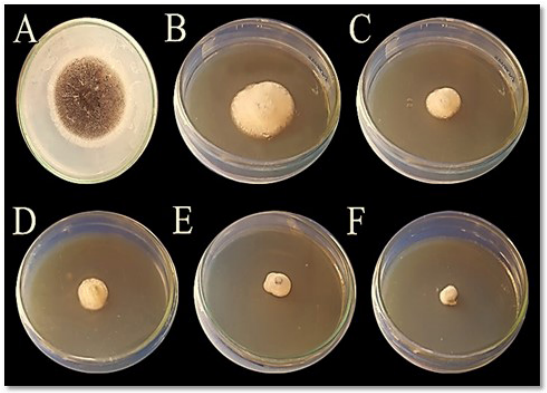

Figure 7. Effect of different concentrations of *C. procera* synthesized silver oxide nanoparticles on fungal growth (A) control, (B) 0.1mg/mL concentration, (C) 0.25mg/mL concentration, (D) 0.5mg/mL concentration, (E) 0.75mg/mL concentration, (F) 1.0mg/mL concentration.

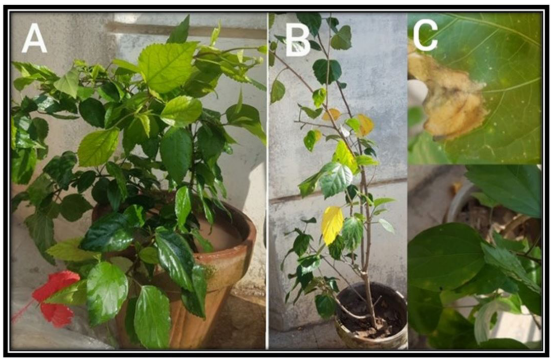

Figure 8. Application of AgNPs on fungal inoculated plants, *in vivo*. Plant with AgNPs application exhibited no fungal leaf spots (A), while control plants exhibited leaf spots symptoms (B) and resulted in leaf necrosis (C).

Table 1. Growth inhibition at different concentrations of AgNPs.

Concentrations (mg/ml)	Growth Inhibition (%)
1.0	87 ± 6.7
0.75	79 ± 5.5
0.5	70 ± 3.5
0.25	59 ± 3.6
0.1	49 ± 2.8
Control	0

3.8. Physiological and biochemical parameters of plants

Study of various physiological parameters (Table 2) and antioxidant enzyme assay (Table 3) assisted to comprehend the defense mechanism of treated plants. Osmo-protectants displayed significant production and remarkable increases in the proline and sugar contents were observed in AgNPs treated plants, when compared with control plants. Protein content varied among all the treatments and the highest protein contents were observed in T_3. Contents of chlorophyll a, chlorophyll b and carotenoids were also increased in T_3 plants, while the lowest contents were observed in T_2 plants. Application of AgNPs increased RWC in T_3 plants and resulted in least electrolyte leakage, among all treatments. Antioxidant enzyme assays depicted distinct variation in the accumulation of enzymes. AgNPs treated plants exhibited higher accumulation of both SOD and POD.

4. Discussion

Agricultural commodities face various pathogenic and abiotic stresses. For the prevention and control of biotic diseases, chemical pesticides are the most used materials. These chemicals can quickly kill the pathogens but they also possess hazardous effects on environment and disturbs human health. Researchers in the agriculture field are focusing on the alternative methods of pesticides. Nanotechnology has become an emerging field to replace chemical applications on plants. They pose less harm to human and animals and provide health friendly control of plant diseases (Jo et al., 2009).

In this study, *C. procera* leaf extract was used for the synthesis of AgNPs. By mixing *C. procera* plant extract with $AgNO_3$ solution, a color shift was detected, indicating actual reduction process. Aqueous extract of *C. procera* did capping and reduction of AgNPs. Designation of brown color surface plasmons are the typical characteristics of AgNPs (Ahmad et al., 2003; Valodkar et al., 2011). UV results of AgNPs depicted the reduction of silver ions, due to release of proteins in the solution of *C. procera* (Ahmad et al., 2011). XRD analysis revealed excellent size of AgNPs (~ 32.43 nm). Nanoparticles have a concentration-dependent impact on plants. NPs concentration influences several plant activities like growth, flowering etc. Small particle size of AgNPs is the key reason of their tremendous antifungal potential, which allows them to penetrate into the leaves during the treatment period and express its growth-enhancing capabilities. AgNPs have been reported to show significant antimicrobial activities against different fungi (*Trichophyton rubrum*, *Candida albicans*, *Aspergillus*

Table 2. Study of physiological parameters in three different treatments.

Treatments	Sugar (µg/g)	Protein (µg/g)	Proline (µg/g)	Chlorophyll a (µg^{-1}/mL)	Chlorophyll b (µg^{-1}/mL)	Carotenoids (µg^{-1}/mL)	RWC (%)	REL (%)
Control (T_1)	384±30.1	54±4.7	124±7.2	0.036±0.004	0.12±0.007	41±2.3	0.12±0.007	79±3.1
Diseased (T_2)	458±32.2	30±	270±15.2	0.013±0.005	0.027±0.005	28±1.1	0.027±0.005	87±4.8
AgNPs Treated (T_3)	855±55.7	68±2.8	420±13.3	0.07±0.003	0.206±0.009	75±1.7	0.206±0.009	77±3.7

Table 3. Estimation of antioxidant enzymes in three different treatments.

Treatments	SOD	POD
Control (T_1)	0.25 ± 0.05	1.3 ± 0.2
Diseased (T_2)	1.173 ± 0.08	2.1 ± 0.05
AgNPs Treated (T_3)	2.12 ± 0.04	2.58 ± 0.11

terreus) and Gram-negative bacteria (*Escherichia coli*, *Pseudomonas aeruginosa*, *Serratia sp*.) (Mohamed et al., 2014). In this study, fungal growth inhibition increased with the increase in AgNPs concentration. It is due to the high density at which solution could adhere and deactivate the pathogenic fungus. This study showed that AgNPs concentration use is less toxic and very effective for anti-fungal application on different plants. Mechanisms responsible for the fungicidal activity of AgNPs include cell membrane damage and the production of reactive oxygen species (ROS). AgNPs attach with cell membrane and destroy spore structure. Silver ions react with thiol group of enzymes and deactivate them. Generation of ROS results in the inhibition of respiratory enzymes via silver ions and destroy cell (Matsumura et al., 2003). AgNPs have been reported to deactivate the replication capability of microorganisms (Feng et al., 2000), which results in deactivating the expression of ribosomal and several other proteins. *C. procera* mediated AgNPs has been used to shield crops from a variety of plant diseases, as an efficient alternative to chemicals.

Green house inoculation assay confirmed the disease control ability of AgNPs. Treated plants showed no disease symptoms, when compared with control. NPs therapies result in the accumulation of minerals that promotes chlorophyll formation, and enzyme stimulation for carbon fixation. NPs increase the photosynthetic rate to stimulates the growth and yield of plants (Tamura et al., 2004) AgNPs have been reported to increase the levels of chlorophyll a, b and carotenoids in *Brassica juncea* (L). leaves due to increased quantum efficiency of PS II (Djurfeldt et al., 2010; Mirzajani et al., 2013). Increased plastid pigments production in AgNPs treated plant is due to improved electron transport (Giraldo et al., 2014). Pigments content increases with the increase in NP concentration (Khodakovskaya et al., 2009) AgNPs application increased sugar content, which are important in the synthesis of defense related lignin and callose (Khizar et al., 2021). Proline content is also produced under stress condition and works as a great osmo-regulator (Alexieva et al., 2001). Application of AgNPs improved the osmoregulation of stressed plants and helped them to bear these conditions.

5. Conclusion and future prospective

Present study has suggested an inexpensive, environment friendly and very effective method of synthesizing AgNPs, using the extract of *C. procera*. These AgNPs can tremendously control leaf spot disease by improving the osmoregulation of diseased plants. Application of AgNPs helped plants to accumulate greater amounts of sugar and proline. Against phyto-pathogenic fungi, AgNPs can be used as a bio-fungicide to protect plants. The findings of our study proved that the green AgNPs could become a new technology for sustainable control of plant diseases.

Acknowledgements

This study was supported by university research fund (URF-20), Quaid-i-Azam University, Islamabad. The authors extend their appreciation to the Deanship of Scientific Research, King Khalid University, for funding this work through research groups program under grant number R.G.P. 2/17/43.

References

AHMAD, A., MUKHERJEE, P., SENAPATI, S., MANDAL, D., KHAN, M.I., KUMAR, R. and SASTRY, M., 2003. Extracellular biosynthesis of silver nanoparticles using the fungus *Fusarium oxysporum*. *Colloids and Surfaces B: Biointerfaces*, vol. 28, no. 4, pp. 313-318. http://dx.doi.org/10.1016/S0927-7765(02)00174-1.

AHMAD, N., SHARMA, S., SINGH, V., SHAMSI, S., FATMA, A. and MEHTA, B., 2011. Biosynthesis of silver nanoparticles from Desmodium triflorum: a novel approach towards weed utilization. *Biotechnology Research International*, vol. 2011, p. 454090. http://dx.doi.org/10.4061/2011/454090. PMid:21350660.

ALEXIEVA, V., SERGIEV, I., MAPELLI, S. and KARANOV, E., 2001. The effect of drought and ultraviolet radiation on growth and stress markers in pea and wheat. *Plant, Cell & Environment*, vol. 24, no. 12, pp. 1337-1344. http://dx.doi.org/10.1046/j.1365-3040.2001.00778.x.

ALI, E.M. and ABDALLAH, B.M., 2020. Effective inhibition of candidiasis using an eco-friendly leaf extract of Calotropis-gigantean-mediated silver nanoparticles. *Nanomaterials*, vol. 10, no. 3, p. 422. http://dx.doi.org/10.3390/nano10030422. PMid:32121137.

AMIN, A., ZAHRA, T., RAJA, H., AMIN, M., DILSHAD, E., NAVEED, M. and AHMED, I., 2020. Major natural sinks for harboring microorganisms with altered antibiotic resistance versus major human contributing sources of antibiotic resistance: a detailed insight. In: M.Z. Hashmi, ed. *Antibiotics and antimicrobial resistance genes in the environment*. Amsterdam: Elsevier, vol. 1, pp. 70-98. http://dx.doi.org/10.1016/B978-0-12-818882-8.00005-X.

ANVAR, M.A., ZOKIRJON, B.U. and RASULJON, R.A., 2021. Main diseases of conclusion trees and measures against them. In: *4th Global Congress on Contemporary Sciences & Advancements*, 30 April 2021, Rome, Italy. Rome: Conference Globe, pp. 99-101.

ARAVIND, M., AHMAD, A., AHMAD, I., AMALANATHAN, M., NASEEM, K., MARY, S., PARVATHIRAJA, C., HUSSAIN, S., ALGARNI, T.S., PERVAIZ, M. and ZUBER, M., 2021. Critical green routing synthesis of silver NPs using jasmine flower extract for biological activities and photocatalytical degradation of methylene blue. *Journal of Environmental Chemical Engineering*, vol. 9, no. 1, p. 104877. http://dx.doi.org/10.1016/j.jece.2020.104877.

BAO, Y., HE, J., SONG, K., GUO, J., ZHOU, X. and LIU, S., 2021. Plant-extract-mediated synthesis of metal nanoparticles. *Journal of Chemistry*, vol. 2021, p. 6562687. http://dx.doi.org/10.1155/2021/6562687.

BATES, L.S., WALDREN, R.P. and TEARE, I., 1973. Rapid determination of free proline for water-stress studies. *Plant and Soil*, vol. 39, no. 1, pp. 205-207. http://dx.doi.org/10.1007/BF00018060.

BEAUCHAMP, C. and FRIDOVICH, I., 1971. Superoxide dismutase: improved assays and an assay applicable to acrylamide gels. *Analytical Biochemistry*, vol. 44, no. 1, pp. 276-287. http://dx.doi.org/10.1016/0003-2697(71)90370-8. PMid:4943714.

BEGUM, Z., YOUNUS, I. and ALI, S., 2015. Anti-inflammatory, analgesic and anti-pyretic activities of Hibiscus rosa-sinesnsis Linn and phytochemicals. *World Journal of Pharmacy and Pharmaceutical Sciences*, vol. 4, no. 12, pp. 116-123.

CHASE, A., 1986. Comparison of three bacterial leaf spots of *Hibiscus rosa-sinensis. Plant Disease*, vol. 70, no. 4, pp. 334-336. http://dx.doi.org/10.1094/PD-70-334.

COHN, B.A., WOLFF, M.S., CIRILLO, P.M. and SHOLTZ, R.I., 2007. DDT and breast cancer in young women: new data on the significance of age at exposure. *Environmental Health Perspectives*, vol. 115, no. 10, pp. 1406-1414. http://dx.doi.org/10.1289/ehp.10260. PMid:17938728.

DEY, J. P., 1978. Fruticose and foliose lichens of the high-mountain areas of the southern Appalachians. *Bryologist*, vol. 81, no. 1, pp. 1-93.

DJURFELDT, M., HJORTH, J., EPPLER, J.M., DUDANI, N., HELIAS, M., POTJANS, T.C., BHALLA, U.S., DIESMANN, M., KOTALESKI, J.H. and EKEBERG, Ö., 2010. Run-time interoperability between neuronal network simulators based on the MUSIC framework. *Neuroinformatics*, vol. 8, no. 1, pp. 43-60. http://dx.doi.org/10.1007/s12021-010-9064-z. PMid:20195795.

FENG, Q.L., WU, J., CHEN, G.Q., CUI, F., KIM, T. and KIM, J., 2000. A mechanistic study of the antibacterial effect of silver ions on Escherichia coli and Staphylococcus aureus. *Journal of Biomedical Materials Research*, vol. 52, no. 4, pp. 662-668. http://dx.doi.org/10.1002/1097-4636(20001215)52:4<662::AID-JBM10>3.0.CO;2-3. PMid:11033548.

GHOSH, P., MANDAL, D., LAHA, S. and DASGUPTA, M., 2009. Dynamics and severity model in managing fungal diseases. *Journal of Plant Protection Sciences*, vol. 1, no. 1, pp. 55-59.

GIRALDO, J.P., LANDRY, M.P., FALTERMEIER, S.M., MCNICHOLAS, T.P., IVERSON, N.M., BOGHOSSIAN, A.A., REUEL, N.F., HILMER, A.J., SEN, F., BREW, J.A. and STRANO, M.S., 2014. Plant nanobionics approach to augment photosynthesis and biochemical sensing. *Nature Materials*, vol. 13, no. 4, pp. 400-408. http://dx.doi.org/10.1038/nmat3890. PMid:24633343.

GORIN, N. and HEIDEMA, F.T., 1976. Peroxidase activity in Golden Delicious apples as a possible parameter of ripening and senescence. *Journal of Agricultural and Food Chemistry*, vol. 24, no. 1, pp. 200-201. http://dx.doi.org/10.1021/jf60203a043. PMid:1245669.

HAHM, M.S., SON, J.S., HWANG, Y.J., KWON, D.K. and GHIM, S.Y., 2017. Alleviation of salt stress in pepper (*Capsicum annum* L.) plants by plant growth-promoting rhizobacteria. *Journal of Microbiology and Biotechnology*, vol. 27, no. 10, pp. 1790-1797. http://dx.doi.org/10.4014/jmb.1609.09042. PMid:28783895.

HAMELIAN, M., HEMMATI, S., VARMIRA, K. and VEISI, H., 2018. Green synthesis, antibacterial, antioxidant and cytotoxic effect of gold nanoparticles using Pistacia Atlantica extract. *Journal of the Taiwan Institute of Chemical Engineers*, vol. 93, pp. 21-30. http://dx.doi.org/10.1016/j.jtice.2018.07.018.

HASSANZADEH, M., EBADI, A., PANAHYAN-E-KIVI, M., ESHGHI, A., JAMAATI-E-SOMARIN, S., SAEIDI, M. and ZABIHI-E-MAHMOODABAD, R., 2009. Evaluation of drought stress on relative water content and chlorophyll content of sesame (*Sesamum indicum* L.) genotypes at early flowering stage. *Research Journal of Environmental Sciences*, vol. 3, no. 3, pp. 345-350. http://dx.doi.org/10.3923/rjes.2009.345.350.

JIN, J., LEE, Y.K. and WICKES, B., 2004. Simple chemical extraction method for DNA isolation from Aspergillus fumigatus and other *Aspergillus* species. *Journal of Clinical Microbiology*, vol. 42, no. 9, pp. 4293-4296. http://dx.doi.org/10.1128/JCM.42.9.4293-4296.2004. PMid:15365025.

JO, Y.K., KIM, B.H. and JUNG, G., 2009. Antifungal activity of silver ions and nanoparticles on phytopathogenic fungi. *Plant Disease*, vol. 93, no. 10, pp. 1037-1043. http://dx.doi.org/10.1094/PDIS-93-10-1037. PMid:30754381.

KAINAMA, H., FATMAWATI, S., SANTOSO, M., PAPILAYA, P.M. and ERSAM, T., 2020. The relationship of free radical scavenging and total phenolic and flavonoid contents of Garcinia lasoar PAM. *Pharmaceutical Chemistry Journal*, vol. 53, no. 12, pp. 1151-1157. http://dx.doi.org/10.1007/s11094-020-02139-5.

KAPOOR, M., KAUR, G., KAUR, N., SHARMA, C., BATRA, K. and SINGH, D., 2021. The traditional uses, phytochemistry and pharmacology of Genus Hibiscus: a review. *European Journal of Medicinal Plants*, vol. 32, no. 4, pp. 1-37. http://dx.doi.org/10.9734/ejmp/2021/v32i430382.

KHAN, M., KHAN, A.U., HASAN, M.A., YADAV, K.K., PINTO, M., MALIK, N., YADAV, V.K., KHAN, A.H., ISLAM, S. and SHARMA, G.K., 2021. Agro-nanotechnology as an emerging field: a novel sustainable approach for improving plant growth by reducing biotic stress. *Applied Sciences*, vol. 11, no. 5, p. 2282. http://dx.doi.org/10.3390/app11052282.

KHANDELWAL, V.K.M., BALARAMAN, R., PANCZA, D. and RAVINGEROVÁ, T., 2011. Hemidesmus indicus and *Hibiscus rosa-sinensis* affect ischemia reperfusion injury in isolated rat hearts. *Evidence-Based Complementary and Alternative Medicine*, vol. 2011, p. 802937. PMid:20953394.

KHIZAR, M., HAROON, U., ALI, M., ARIF, S., SHAH, I.H., CHAUDHARY, H.J. and MUNIS, M.F.H., 2020. Aspergillus tubingensis causes leaf spot of cotton (*Gossypium hirsutum* L.) in Pakistan. *Phyton*, vol. 89, no. 1, p. 103.

KHIZAR, M., HAROON, U., KAMAL, A., INAM, W., CHAUDHARY, H.J. and MUNIS, M.F.H., 2021. Evaluation of virulence potential of *Aspergillus tubingensis* and subsequent biochemical and enzymatic defense response of cotton. *Microscopy Research and Technique*, vol. 84, no. 11, pp. 2694-2701. http://dx.doi.org/10.1002/jemt.23832. PMid:34002427.

KHODAKOVSKAYA, M., DERVISHI, E., MAHMOOD, M., XU, Y., LI, Z., WATANABE, F. and BIRIS, A.S., 2009. Carbon nanotubes are able to penetrate plant seed coat and dramatically affect seed germination and plant growth. *ACS Nano*, vol. 3, no. 10, pp. 3221-3227. http://dx.doi.org/10.1021/nn900887m. PMid:19772305.

LECOMTE, C., ALABOUVETTE, C., EDEL-HERMANN, V., ROBERT, F. and STEINBERG, C., 2016. Biological control of ornamental plant diseases caused by Fusarium oxysporum: a review. *Biological Control*, vol. 101, pp. 17-30. http://dx.doi.org/10.1016/j.biocontrol.2016.06.004.

LIAQUAT, F., MUNIS, M., ARIF, S., CHE, S. and LIU, Q., 2019. Presence of *Aspergillus tubingensis* causing leaf spot disease of Helleborus species in Shanghai, China. *Plant Disease*, vol. 103, no. 4, p. 766. http://dx.doi.org/10.1094/PDIS-07-18-1226-PDN.

LOWRY, O.H., ROSEBROUGH, N.J., FARR, A.L. and RANDALL, R.J., 1951. Protein measurement with the Folin phenol reagent. *The Journal of Biological Chemistry*, vol. 193, no. 1, pp. 265-275. http://dx.doi.org/10.1016/S0021-9258(19)52451-6. PMid:14907713.

LUTTS, S., KINET, J. and BOUHARMONT, J., 1996. NaCl-induced senescence in leaves of rice (*Oryza sativa* L.) cultivars differing

in salinity resistance. *Annals of Botany*, vol. 78, no. 3, pp. 389-398. http://dx.doi.org/10.1006/anbo.1996.0134.

MADKOUR, L.H., 2019. *Nanoelectronic materials: fundamentals and applications*. Cham: Springer Nature. Introduction to nanotechnology (NT) and nanomaterials (NMs), pp. 1-47, Advanced Structured Materials. http://dx.doi.org/10.1007/978-3-030-21621-4_1.

MATSUMURA, Y., YOSHIKATA, K., KUNISAKI, S.-I. and TSUCHIDO, T., 2003. Mode of bactericidal action of silver zeolite and its comparison with that of silver nitrate. *Applied and Environmental Microbiology*, vol. 69, no. 7, pp. 4278-4281. http://dx.doi.org/10.1128/AEM.69.7.4278-4281.2003. PMid:12839814.

MIRZAJANI, F., ASKARI, H., HAMZELOU, S., FARZANEH, M. and GHASSEMPOUR, A., 2013. Effect of silver nanoparticles on *Oryza sativa* L. and its rhizosphere bacteria. *Ecotoxicology and Environmental Safety*, vol. 88, pp. 48-54. http://dx.doi.org/10.1016/j.ecoenv.2012.10.018. PMid:23174269.

MOHAMED, N.H., ISMAIL, M.A., ABDEL-MAGEED, W.M. and SHOREIT, A.A.M., 2014. Antimicrobial activity of latex silver nanoparticles using *Calotropis procera. Asian Pacific Journal of Tropical Biomedicine*, vol. 4, no. 11, pp. 876-883. http://dx.doi.org/10.12980/APJTB.4.201414B216.

PARVATHI, V.P., UMADEVI, M., SASIKALA, R., PARIMALADEVI, R., RAGAVENDRAN, V., MAYANDI, J. and SATHE, G., 2020. Novel silver nanoparticles/activated carbon co-doped titania nanoparticles for enhanced antibacterial activity. *Materials Letters*, vol. 258, p. 126775. http://dx.doi.org/10.1016/j.matlet.2019.126775.

PATTNAIK, P.K., KAR, D., CHHATOI, H., SHAHBAZI, S., GHOSH, G. and KUANAR, A., 2017. Chemometric profile & antimicrobial activities of leaf extract of *Calotropis procera* and Calotropis gigantea. *Natural Product Research*, vol. 31, no. 16, pp. 1954-1957. http://dx.doi.org/10.1080/14786419.2016.1266349. PMid:27936921.

PINTO, M.M.S.C., MARINHO-REIS, P., ALMEIDA, A., PINTO, E., NEVES, O., INÁCIO, M., GERARDO, B., FREITAS, S., SIMÕES, M.R., DINIS, P.A., DINIZ, L., SILVA, E.F. and MOREIRA, P.I., 2019. Links between cognitive status and trace element levels in hair for an environmentally exposed population: a case study in the surroundings of the estarreja industrial area. *International Journal of Environmental Research and Public Health*, vol. 16, no. 22, p. 4560. http://dx.doi.org/10.3390/ijerph16224560. PMid:31752166.

PUNJA, Z.K., 2006. Recent developments toward achieving fungal disease resistance in transgenic plants. *Canadian Journal of Plant Pathology*, vol. 28, suppl. 1, pp. S298-S308. http://dx.doi.org/10.1080/07060660609507387.

RAZAVI, M.E., SALAHINEJAD, E., FAHMY, M., YAZDIMAMAGHANI, M., VASHAEE, D. and TAYEBI, L., 2015. Green chemical and biological synthesis of nanoparticles and their biomedical applications. In: V. Basiuk and E. Basiuk, eds. *Green processes for nanotechnology*. Cham, Springer, pp. 207-235. http://dx.doi.org/10.1007/978-3-319-15461-9_7.

SAFA, M.M., MEROUANE, M.F., HOUDA, M.C., GOLZADEH, N., VASSEGHIAN, Y. and BERKANI, M., 2021. Biosynthesis, characterization, and evaluation of antibacterial and photocatalytic methylene blue dye degradation activities of silver nanoparticles from Streptomyces tuirus strain. *Environmental Research*, vol. 204, no. Pt D, p. 112360.

SANCI, R. and VOLKAN, M., 2009. Surface-enhanced Raman scattering (SERS) studies on silver nanorod substrates. *Sensors and Actuators B: Chemical*, vol. 139, no. 1, pp. 150-155. http://dx.doi.org/10.1016/j.snb.2008.10.033.

SHARMA, S., KOTA, K. and PANDYA, N.D., 2021. A study of angiogenic activity of *Hibiscus rosa-sinensis* Linn. using chick chorioallantoic membrane model. *National Journal of Physiology, Pharmacy and Pharmacology*, vol. 11, no. 10, pp. 1080-1084. http://dx.doi.org/10.5455/njppp.2021.11.03094202102052021.

SHELKE, M., PARJANE, S., MANKAR, S. and SIDDHESHWAR, S., 2021. Therapeutic potential of *Hibiscus rosa sinensis*-a review. *Research Journal of Science and Technology*, vol. 13, no. 2, pp. 151-156. http://dx.doi.org/10.52711/2349-2988.2021.00023.

SILVA, M.C.C., SILVA, A.B., TEIXEIRA, F.M., SOUSA, P.C.P., RONDON, R.M.M., HONÓRIO JÚNIOR, J.E.R., SAMPAIO, L.R.L., OLIVEIRA, S.L., HOLONDA, A.N.M. and VASCONCELOS, S.M.M., 2010. Therapeutic and biological activities of *Calotropis procera* (Ait.). *Asian Pacific Journal of Tropical Medicine*, vol. 3, no. 4, pp. 332-336. http://dx.doi.org/10.1016/S1995-7645(10)60081-8.

SIVARAMAN, C.M. and SAJU, F., 2021. Medicinal value of Hibiscus rosa sinensis: a review. *International Journal of Pharmacognosy and Chemistry*, vol. 2, no. 1, pp. 1-11. http://dx.doi.org/10.46796/ijpc.vi.128.

STOCKBURGER, K.A. and MITCHELL, A.K., 1999. *Photosynthetic pigments: a bibliography*. Victoria: Pacific Forestry Centre, vol. 383, 38 p.

SUSCA, A., STEA, G., MULÉ, G. and PERRONE, G., 2007. Polymerase chain reaction (PCR) identification of Aspergillus niger and Aspergillus tubingensis based on the calmodulin gene. *Food Additives and Contaminants*, vol. 24, no. 10, pp. 1154-1160. http://dx.doi.org/10.1080/02652030701546206. PMid:17886188.

TAMBURINI, G., PEREIRA-PEIXOTO, M.H., BORTH, J., LOTZ, S., WINTERMANTEL, D., ALLAN, M.J., DEAN, R., SCHWARZ, J.M., KNAUER, A., ALBRECHT, M. and KLEIN, A.M., 2021. Fungicide and insecticide exposure adversely impacts bumblebees and pollination services under semi-field conditions. *Environment International*, vol. 157, p. 106813. http://dx.doi.org/10.1016/j.envint.2021.106813. PMid:34455190.

TAMURA, K., NEI, M. and KUMAR, S., 2004. Prospects for inferring very large phylogenies by using the neighbor-joining method. *Proceedings of the National Academy of Sciences of the United States of America*, vol. 101, no. 30, pp. 11030-11035. http://dx.doi.org/10.1073/pnas.0404206101. PMid:15258291.

TANIGUCHI, N., 1974. On the basic concept of nano-technology. In: *Proceedings of the International Conference on Production Engineering*, 26-29 August 1974, Tokyo, Japan. Tokyo: Japan Society of Precision Engineering, pp. 18-23.

VALODKAR, M., NAGAR, P.S., JADEJA, R.N., THOUNAOJAM, M.C., DEVKAR, R.V. and THAKORE, S., 2011. Euphorbiaceae latex induced green synthesis of non-cytotoxic metallic nanoparticle solutions: a rational approach to antimicrobial applications. *Colloids and Surfaces. A, Physicochemical and Engineering Aspects*, vol. 384, no. 1-3, pp. 337-344. http://dx.doi.org/10.1016/j.colsurfa.2011.04.015.

VERMA, A. and BHARADVAJA, N., 2021. Plant-mediated synthesis and characterization of silver and copper oxide nanoparticles: antibacterial and heavy metal removal activity. *Journal of Cluster Science*, pp. 1-16 http://dx.doi.org/10.1007/s10876-021-02091-8. In Press.

VETTER, J., STEINBERG, M. and NELSON, A., 1958. Enzyme assay, quantitative determination of peroxidase in sweet corn. *Journal of Agricultural and Food Chemistry*, vol. 6, no. 1, pp. 39-41. http://dx.doi.org/10.1021/jf60083a006.

WANG, Z.L., 2000. Transmission electron microscopy and spectroscopy of nanoparticles. *Characterization of Nanophase Materials*, vol. 3, pp. 37-80.

WEATHERLEY, P., 1950. Studies in the water relations of cotton plants. I. The field measurement of water deficit in leaves. *The New Phytologist*, vol. 49, no. 1, pp. 81-97. http://dx.doi.org/10.1111/j.1469-8137.1950.tb05146.x.